Electric quadrupole and magnetic dipole transition probabilities in the potassium isoelectronic sequence

M. A. Ali
Chemistry Department, Howard University, Washington, D.C. 20059

Yong-Ki Kim
National Bureau of Standards, Gaithersburg, Maryland 20899
(Received 22 February 1988)

Electric quadrupole and magnetic dipole transition probabilities between the $3p^6 4s\ ^2S_{1/2}$ and the $3p^6 3d\ ^2D_{3/2}$, $^2D_{5/2}$ levels for K through Mo^{23+} have been calculated in the (relativistic) Dirac-Fock single-configuration approximation. The positions of the (excited) $4s\ ^2S_{1/2}$ level for Mn^{7+}-Mo^{23+} are predicted along with the fine-structure splitting in the ground configuration $3p^6 3d$.

I. INTRODUCTION

Theoretical studies of atomic transition probabilities have mostly concentrated on dipole-allowed transitions, as these are usually responsible for strong lines in atomic spectra. However, it is now realized that under conditions which obtain in astrophysical and low-density laboratory tokamak plasmas where collisional deexcitation of metastable states is rather slow leading to buildup of population of metastable levels, forbidden transitions, i.e., electric quadrupole and magnetic dipole transitions, gain in intensity and can be used to infer information about plasma temperature and dynamics.[1-6] Furthermore, electric quadrupole transition probabilities increase as Z^6 and Z for interconfiguration and intraconfiguration transitions, respectively, where Z is the nuclear charge. Magnetic dipole transition probability increases as Z^6 and Z^3 for interconfiguration and intraconfiguration transitions, respectively, if electron-electron Coulomb repulsion is the dominant mechanism for energy-level separation. For intraconfiguration transitions between levels, the separation of which is primarily due to spin-orbit effects, magnetic dipole transition probability increases as Z^{12}. Thus along an isoelectronic sequence the ratio of probabilities for dipole-forbidden and dipole-allowed transitions may slowly increase with increasing nuclear charge.[7]

Kaufman and Sugar[8] have recently published a compilation of forbidden lines and transition probabilities arising from the ns^2np^k configurations for $n=2$ and 3. Gauthier *et al.*[9] have recently identified and classified electric quadrupole transitions in the spectra of neonlike ions produced by laser irradiation. Godefroid *et al.*[10] in fact suggest that forbidden lines might be more prevalent and have been recorded in old and current plates more than has been noticed by spectroscopists. On the theoretical front a variety of models ranging from Hartree-Fock, multiconfiguration Hartree-Fock, multiconfiguration Dirac-Fock, and configuration mixing[11-19] have been used to calculate electric quadrupole and magnetic dipole transition probabilities.

Although much attention has been devoted to the calculation of electric quadrupole transition probabilities for the sodium isoelectronic sequence,[10-13] very little work has been done to calculate similar quantities for the potassium isoelectronic sequence.[13] Spectra of members of the potassium isoelectronic sequence such as Zn^{11+}, Se^{15+}, and Mo^{23+} have already been generated and studied in laboratory plasmas, and higher members such as Xe^{35+} are likely to be generated and studied soon. However, very little is known experimentally or theoretically about energy-level structure and allowed and forbidden transition probabilities in such systems. Knowledge of electric quadrupole and magnetic dipole transition energies and probabilities for the potassium isoelectronic sequence would be useful in identifying forbidden lines in tokamak plasmas and other laboratory produced plasmas. The present study is the first part of a general study to fill this gap.

II. PRESENT WORK

The energy levels of the potassium isoelectronic sequence currently known[20] have been tabulated through Ni^{9+}. The ground level in K is $4s\ ^2S_{1/2}$ followed by $4p\ ^2P_{1/2,3/2}$, $5s\ ^2S_{1/2}$, $3d\ ^2D_{3/2,5/2}$. In Ca^+ the levels $3d\ ^2D_{3/2,5/2}$ move down to be the excited levels next to the ground-level $4s\ ^2S_{1/2}$. For Sc^{2+} to Cr^{5+}, $3d\ ^2D_{3/2,5/2}$ are the lowest levels followed by the $4s\ ^2S_{1/2}$ level. For higher members of the sequence, $3d\ ^2D_{3/2,5/2}$ are the lowest levels followed by core excited and other odd-parity levels, and the $4s\ ^2S_{1/2}$ level has not been identified at all. In fact from Mn^{6+} onwards, no other even-parity level besides the ground level has been identified.

In K the decay of $3d\ ^2D_{3/2,5/2}$ to $4s\ ^2S_{1/2}$ by electric quadrupole and magnetic dipole transitions is in competition with electric dipole transition to $4p\ ^2P_{1/2,3/2}$ and then to $4s\ ^2S_{1/2}$. In Ca^+ to Cr^{6+}, $4s\ ^2S_{1/2}$ and $3d\ ^2D_{3/2,5/2}$ are adjacent to each other, and the decay possible from the upper level is by magnetic dipole and electric quadrupole transitions.[21] In Sc^{2+} to Cr^{6+}, the $4s\ ^2S_{1/2}$ level can decay to either the $3d\ ^2D_{3/2}$ or $3d\ ^2D_{5/2}$ level by electric quadrupole transitions, fol-

lowed by the decay of the $3d\ ^2D_{5/2}$ level to the $3d\ ^2D_{3/2}$ level by magnetic dipole and electric quadrupole transitions.[21] These are shown schematically in Fig. 1. From Mn^{6+} and beyond, the $4s\ ^2S_{1/2}$ level has not been identified. In fact, no other even-parity level besides the ground level has been identified. Hertel and Ross[22] have experimentally determined quadrupole Einstein coefficients for K along with those for Na, Rb, and Cs from electron-impact spectra. Their value for K is two to three times larger than that calculated in the Hartree-Fock or Coulomb approximation or Hartree-Fock plus core-valence configuration interaction.[13] No other theoretical result is available for other members of the K sequence.

We have used single relativistic configuration wave functions for the $4s\ ^2S_{1/2}$ and $3d\ ^2D_{3/2,5/2}$ levels generated by an advanced version of the multiconfiguration Dirac-Fock (MCDF) program of Desclaux[23] in optimized level mode (i.e., Dirac-Fock radial functions are chosen to minimize the energy of each level separately) to calculate the transition energies and line strengths. Among other improvements, this code includes QED corrections for $n \geq 3$ electrons that also take into account the screening of the nuclear charge by bound electrons. QED effects become the major source of uncertainties in transition energies for $Z > 30$.

Since the model wave function is rather simple with no correlation of the core electrons included, the calculated transition energies are not reliable for the low-Z members of the isoelectronic sequence. However, the accuracy of the transition energy is likely to improve as the nuclear charge increases. In Table I we compare $\Delta E_{\text{theor}}(4s\ ^2S_{1/2}-3d\ ^2D_{3/2})$ calculated by our single-configuration Dirac-Fock model with available experimental values. It is seen that for Cr^{5+} the difference between ΔE_{theor} and ΔE_{expt} is down to 400 cm^{-1}. Thus we can predict the position of the $4s\ ^2S_{1/2}$ level relative to the $3d\ ^2D_{3/2}$ level with some confidence from Mn^{6+} onwards. Such theoretical transition energies are presented also in Table I. Thus in Mn^{6+} and Fe^{7+}, the $4s\ ^2S_{1/2}$ level is the next level closest to the $3d\ ^2D_J$ ground levels and

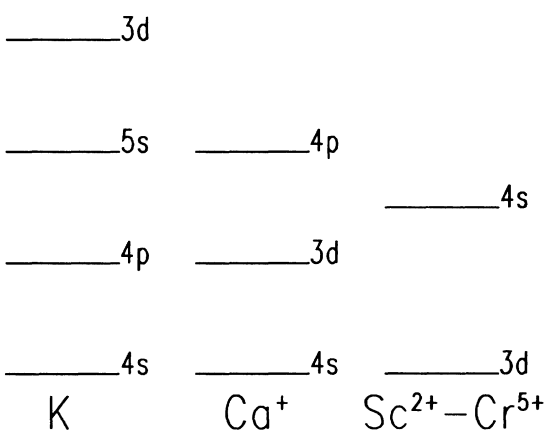

FIG. 1. Schematic energy-level diagram (not to scale) for K to Cr^{5+} showing the metastable nature of the $3d\ ^2D_J$ levels in Ca^+ and the $4s\ ^2S_{1/2}$ level in Sc^{2+}–Cr^{5+}.

TABLE I. Comparison of the theoretical and experimental excitation energy from the $3d\ ^2D_{3/2}$ to the $4s\ ^2S_{1/2}$ level (cm^{-1}). Experimental values were taken from Ref. 20.

Atom	Theory	Experiment	Expt.-theory
K	−19 672	−21 537	−1865
Ca^+	−16 547	−13 650	−2897
Sc^{2+}	22 828	25 539	2711
Ti^{3+}	78 432	80 389	1958
V^{4+}	146 974	148 143	1169
Cr^{5+}	227 455	227 858	403

Atom	Theory	Atom	Theory
Mn^{6+}	319 400	Se^{15+}	1 635 400
Fe^{7+}	422 500	Br^{16+}	1 834 400
Co^{8+}	536 700	Kr^{17+}	2 043 800
Ni^{9+}	661 700	Rb^{18+}	2 263 400
Cu^{10+}	797 500	Sr^{19+}	2 493 400
Zn^{11+}	944 000	Y^{20+}	2 733 600
Ga^{12+}	1 101 100	Zr^{21+}	2 984 000
Ge^{13+}	1 268 700	Nb^{22+}	3 244 500
As^{14+}	1 446 800	Mo^{23+}	3 515 100

the $4s\ ^2S_{1/2}$ level is truly metastable, while in Co^{8+} and Ni^{9+}, core ($3p$) excited odd-parity levels of the $3p^53d^2$ configuration with different J values starting from $\frac{1}{2}$ intervene between the $3p^64s\ ^2S_{1/2}$ and the $3p^63d\ ^2D_J$ levels. According to the identifications made by Ramonas and Ryabtsev[20,24] and our calculated transition energies (Table I), the $3p^5(^2P^o)3d^2(^1G)\ ^2F^o_{5/2}$, $^2F^o_{7/2}$, $3p^5(^2P^o)3d^2(^1D)\ ^2F^o_{7/2}$, $^2F^o_{5/2}$ levels intervene between the $3p^63d\ ^2D_J$ and $3p^64s\ ^2S_{1/2}$ levels in Co^{8+}. Similarly we conclude that the $3p^5(^2P^o)3d^2(^1G)\ ^2F^o_{5/2}$, $^2F^o_{7/2}$, $3p^5(^2P^o)3d^2(^1D)\ ^2F^o_{7/2}$, $^2F^o_{5/2}$, $3p^5(^2P^o)3d^2(^3F)\ ^2F^o_{5/2}$, $^2F^o_{7/2}$ levels intervene between the $3p^63d\ ^2D_J$ levels and the $3p^64s\ ^2S_{1/2}$ level in Ni^{9+}. However, transitions from the $4s\ ^2S_{1/2}$ level to these low-lying $3p^53d^2$ odd-parity levels with $J=\frac{5}{2}$ and $\frac{7}{2}$ would be electric dipole forbidden due to ΔJ selection rules.[25] As the nuclear charge increases, the $3p^53d^2\ J=\frac{1}{2}$ and $\frac{3}{2}$ levels would tend to lie below the $3p^64s\ ^2S_{1/2}$ level in the energy scale. Transitions from the $4s\ ^2S_{1/2}$ level to these low-lying $3p^53d^2\ J=\frac{1}{2}, \frac{3}{2}$ levels are electric dipole allowed. However, these transitions would require changes in the quantum number of two electrons and would thus have rather low transition probabilities. Thus the decay of the $4s\ ^2S_{1/2}$ level by electric quadrupole and magnetic dipole radiation to the $3d\ ^2D_J$ levels might still be the dominant decay mechanism and may compete with the electric dipole decay mode.

In Table II we compare spin-orbit splitting $\Delta E_{\text{theor,s.o.}}(3d\ ^2D_{5/2}-3d\ ^2D_{3/2})$ calculated in the single-configuration approximation with $\Delta E_{\text{expt,s.o.}}$ to test whether the simple, single-configuration approximation with Lamb shift corrections included for the M and N shells also is successful in predicting such splitting. We collect also in Table II calculated theoretical spin-orbit splitting in ions up to Mo^{23+} for some of which no experimental results are available. We see that the spin-orbit

TABLE II. Comparison of the theoretical and experimental spin-orbit splitting between $3d\,^2D_{5/2}$ and $3d\,^2D_{3/2}$ levels (cm^{-1}). Experimental values were taken from Ref. 20 unless indicated otherwise.

Atom	Theory	Experiment	Atom	Theory	Experiment
K	−2.69	−2.31	Ga^{12+}	6244	
Ca^{+}	31	61	Ge^{13+}	7643	
Sc^{2+}	168	197.6	As^{14+}	9255	
Ti^{3+}	354	382.1	Se^{15+}	11 100	11 080[c]
V^{4+}	599	624.9	Br^{16+}	13 200	
Cr^{5+}	913	940	Kr^{17+}	15 576	
Mn^{6+}	1310	1338	Rb^{18+}	18 251	
Fe^{7+}	1804	1836	Sr^{19+}	21 248	
Co^{8+}	2408	2451	Y^{20+}	24 593	
Ni^{9+}	3138	3178	Zr^{21+}	28 312	28 505[d]
Cu^{10+}	4009	4060[a]	Nb^{22+}	32 430	
Zn^{11+}	5039	4956[b]	Mo^{23+}	36 975	37 212[d]

[a]Reference 24.
[b]Reference 26.
[c]Reference 27.
[d]Reference 28.

splitting in the ground configuration is predicted rather well, for K to Zn^{11+}. Thus we expect that the calculated spin-orbit splitting in Ga^{12+} through Mo^{23+}, would be substantially accurate.

In the calculation of line strengths we disregard the difference in spectator orbitals of the different levels and only calculate contributions arising from active orbitals involved in the transition in the length form. It is difficult to estimate the error in line strength arising from this simplification. Nevertheless, we estimate that error is unlikely to be more than 20%. We use the experimental transition energies where available as the transition probabilities depend sensitively on transition energies so that any uncertainty in transition probability is due only to inaccuracy in calculated line strength. Where experimental transition energies are not available, theoretical

TABLE III. Calculated electric quadrupole transition probabilities (A_{E2}) and transition wavelengths (λ) for the $3d\,^2D$–$4s\,^2S$ transitions. For K to Cr^{5+} experimental wavelengths are used. Notation: $1.224(+05)=1.224\times10^{+5}$.

Atom	λ (Å)	A_{E2} (sec^{-1}) ($3d\,^2D_{3/2}$–$4s\,^2S_{1/2}$)	λ (Å)	A_{E2} (sec^{-1}) ($3d\,^2D_{5/2}$–$4s\,^2S_{1/2}$)
K	4644	154	4644	154
Ca^{+}	7326	1.02	7293	1.05
Sc^{2+}	3916	8.21	3946	11.9
Ti^{3+}	1244	8.83(+02)	1250	1.30(+03)
V^{4+}	675.0	8.56(+03)	677.9	1.27(+04)
Cr^{5+}	438.9	3.90(+04)	440.7	5.78(+04)
Mn^{6+}	312.2	1.22(+05)	314.5	1.82(+05)
Fe^{7+}	236.8	3.09(+05)	237.8	4.59(+05)
Co^{8+}	186.4	6.69(+05)	187.2	9.94(+05)
Ni^{9+}	151.2	1.30(+06)	151.9	1.93(+06)
Cu^{10+}	125.4	2.33(+06)	126.1	3.47(+06)
Zn^{11+}	106.0	3.93(+06)	106.5	5.84(+06)
Ga^{12+}	90.82	6.32(+06)	91.34	9.38(+06)
Ge^{13+}	78.82	9.72(+06)	79.30	1.44(+07)
As^{14+}	69.12	1.45(+07)	69.56	2.15(+07)
Se^{15+}	61.15	2.09(+07)	61.56	3.11(+07)
Br^{16+}	54.51	2.95(+07)	54.91	4.38(+07)
Kr^{17+}	48.93	4.07(+07)	49.31	6.04(+07)
Rb^{18+}	44.18	5.52(+07)	44.54	8.18(+07)
Sr^{19+}	40.11	7.36(+07)	40.45	1.09(+08)
Y^{20+}	36.58	9.66(+07)	36.91	1.43(+08)
Zr^{21+}	33.51	1.25(+08)	33.83	1.86(+08)
Nb^{22+}	30.82	1.60(+08)	31.13	2.37(+08)
Mo^{23+}	28.45	2.03(+08)	28.75	3.01(+08)

TABLE IV. Theoretical magnetic dipole transition probabilities (A_{M1}) and experimental or theoretical wavelengths (λ) for the $4s\ ^2S_{1/2}-3d\ ^2D_{3/2}$ transitions.

Atom	λ (Å)	A_{M1} (sec^{-1})
K	4644	8.77(−10)
Ca^+	7326	7.39(−11)
Sc^{2+}	3916	1.05(−08)
Ti^{3+}	1244	5.57(−07)
V^{4+}	675.0	4.21(−06)
Cr^{5+}	438.9	1.56(−05)
Mn^{6+}	313.2	3.85(−05)
Fe^{7+}	236.8	7.06(−05)
Co^{8+}	186.4	9.83(−05)
Ni^{9+}	151.2	9.83(−05)
Cu^{10+}	125.4	5.43(−05)
Zn^{11+}	106.0	9.06(−07)
Ga^{12+}	90.82	1.19(−04)
Ge^{13+}	78.82	8.93(−04)
As^{14+}	69.12	3.40(−03)
Se^{15+}	61.15	9.69(−03)
Br^{16+}	54.51	2.34(−02)
Kr^{17+}	48.93	5.08(−02)
Rb^{18+}	44.18	1.01(−01)
Sr^{19+}	40.11	1.90(−01)
Y^{20+}	36.58	3.40(−01)
Zr^{21+}	33.51	5.83(−01)
Nb^{22+}	30.82	9.66(−01)
Mo^{23+}	28.45	1.55(+00)

TABLE V. Theoretical magnetic dipole (A_{M1}) and electric quadrupole (A_{E2}) transition probabilities and experimental or theoretical transition wavelengths (λ) for the $3d\ ^2D_{5/2}-3d\ ^2D_{3/2}$ transition. Experimental value of A_{M1} for Fe^{7+} is 0.0705 sec^{-1} (Ref. 30). Notation: $4.33(+07)=4.33\times10^{+7}$.

Atom	λ (Å)	A_{M1} (sec^{-1})	A_{E2} (sec^{-1})
K	4.33(+07)	1.99(−10)	7.23(−18)
Ca^+	1.64(+06)	2.45(−06)	2.89(−13)
Sc^{2+}	5.061(+05)	8.32(−05)	1.75(−11)
Ti^{3+}	2.617(+05)	6.02(−04)	1.93(−10)
V^{4+}	1.600(+05)	2.63(−03)	1.19(−09)
Cr^{5+}	1.064(+05)	8.96(−03)	5.53(−09)
Mn^{6+}	7.474(+04)	2.58(−02)	2.10(−08)
Fe^{7+}	5.447(+04)	6.67(−02)	7.04(−08)
Co^{8+}	4.080(+04)	1.59(−01)	2.14(−07)
Ni^{9+}	3.147(+04)	3.46(−01)	5.80(−07)
Cu^{10+}	2.4942(+04)	6.95(−01)	1.41(−06)
Zn^{11+}	1.9846(+04)	1.38	3.41(−06)
Ga^{12+}	1.6016(+04)	2.62	7.85(−06)
Ge^{13+}	1.3084(+04)	4.81	1.73(−05)
As^{14+}	1.0805(+04)	8.54	3.69(−05)
Se^{15+}	9.0089(+03)	1.47(+01)	7.41(−05)
Br^{16+}	7.5759(+03)	2.48(+01)	1.46(−04)
Kr^{17+}	6.4203(+03)	4.07(+01)	2.79(−04)
Rb^{18+}	5.4793(+03)	6.54(+01)	5.20(−04)
Sr^{19+}	4.7063(+03)	1.03(+02)	9.44(−04)
Y^{20+}	4.0661(+03)	1.60(+02)	1.68(−03)
Zr^{21+}	3.5321(+03)	2.44(+02)	2.91(−03)
Nb^{22+}	3.0836(+03)	3.67(+02)	4.97(−03)
Mo^{23+}	2.7045(+03)	5.44(+02)	8.33(−03)

values are used. However, as we have argued earlier, theoretical values are likely to be substantially accurate. The following formulas[29] are used for calculation of transition probabilities:

$$A_{E2}=\frac{(1.1199\times10^{18})S_{E2}}{g_k\lambda^5_{\text{expt}}}\ , \tag{1}$$

$$A_{M1}=\frac{(2.697\times10^{13})S_{M1}}{g_k\lambda^3_{\text{expt}}}\ , \tag{2}$$

where λ_{expt} is the experimental transition wavelength in Å, g_k is the $(2J+1)$ degeneracy of the upper level, S_{M1} is the $M1$ line strength in Bohr magneton units (u_B), and S_{E2} is the $E2$ line strength in atomic units (ea_0^2). The calculated transition probabilities are presented in Tables III–V.

III. DISCUSSION OF RESULTS

Comparison of experimental and calculated transition energies between the $4s\ ^2S_{1/2}$ and $3d\ ^2D_{3/2}$ levels in Table I shows that the correct ordering of levels is predicted even for K and Ca^+ in the simple single-configuration approximation. However, the calculated transition energies for K to Sc^{2+} would be subject to large errors because the energy of these levels varies rapidly with nuclear charge, returning to the hydrogenic level scheme in Sc^{2+}. The difference between calculated and experimental transition energies steadily decreases from Sc^{2+} to Cr^{5+}. At this point calculated transition energies for the higher members of the sequence are expected to be reliable, and we can assign the location of the $4s\ ^2S_{1/2}$ level on the energy scale for the higher members of the sequence.

In Mn^{6+} and Fe^{7+}, the $4s\ ^2S_{1/2}$ level is expected to be immediately above the $3d\ ^2D_{5/2}$ level at 319 400 and 422 500 cm^{-1}, respectively, above the ground-level $3d\ ^2D_{3/2}$. Thus the $4s\ ^2S_{1/2}$ level is metastable in Mn^{6+} and Fe^{7+}. In Co^{8+} two $J=\frac{5}{2}$ and two $J=\frac{7}{2}$ levels arising from $3p^5(^2P^o)3d^2(^1G)$ and $3p^5(^2P^o)3d^2(^1D)$ intervene between the $3d\ ^2D_{3/2,5/2}$ and $4s\ ^2S_{1/2}$ levels.[20] In Ni^{9+}, our results suggest that three $J=\frac{5}{2}$ and three $J=\frac{7}{2}$ levels arising from the $3p^53d^2$ configuration lie between the $3d\ ^2D_{3/2,5/2}$ and $4s\ ^2S_{1/2}$ levels.[20] In Cu^{10+} the $J=\frac{1}{2}$ and $J=\frac{3}{2}$ levels arising from the $3p^53d^2$ configuration and the $J=\frac{5}{2}$ and $J=\frac{7}{2}$ levels arising from the same configuration intervene between the $3d\ ^2D_{3/2,5/2}$ and $4s\ ^2S_{1/2}$ levels.[24] The patterns of energy-level structure as described above are shown schematically in Fig. 2.

In Co^{8+} and Ni^{9+} transition from the $4s\ ^2S_{1/2}$ level to the odd-parity levels below is electric dipole forbidden by the ΔJ selection rule and would involve two-electron orbital changes. Thus in Co^{8+} and Ni^{9+} the $4s\ ^2S_{1/2}$ level is metastable. In Cu^{10+} the $4s\ ^2S_{1/2}$ level can decay in principle to odd parity $J=\frac{1}{2}$ and $J=\frac{3}{2}$ lower-lying levels of the $3p^53d^2$ configuration. However, these transitions would be very weak because they require two-electron orbital changes. This general situation has been discussed by Mansfield *et al.*[25] Very little information is available about the energy-level structure, particularly the core-

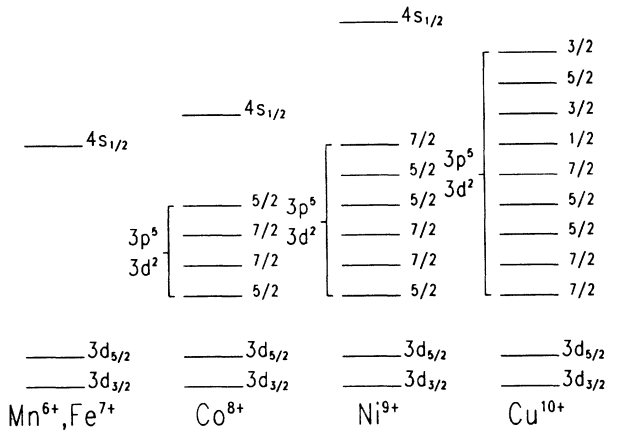

FIG. 2. Schematic energy-level diagram (not to scale) for Mn^{6+} to Cu^{10+} according to our calculated results and energy-level data in Refs. 20 and 24 suggesting that the $4s\ ^2S_{1/2}$ level is metastable in Mn^{6+} and Fe^{7+} and weakly electric dipole allowed in Co^{8+} to Cu^{10+}.

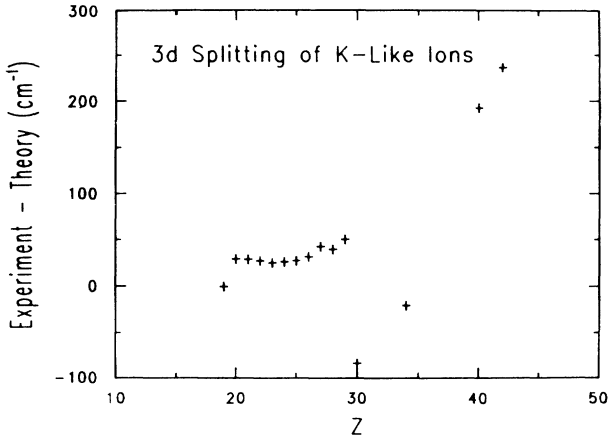

FIG. 3. The difference between the experimental and calculated fine-structure splitting as a function of nuclear charge Z. The difference is approximately constant for $Z \leq 25$, which suggests that the difference is mainly due to electron correlation. For $Z \geq 30$, the difference rises with increasing Z indicating that higher-order relativistic effects dominate. The experimental values for Zn^{11+} and Se^{15+} seem to be too low.

excited odd-parity levels of the higher members of the K isoelectronic sequence. We are presently engaged in investigating these energy levels, particularly odd-parity core-excited levels of the K isoelectronic sequence by the MCDF method.

A glance at Table II shows that the spin-orbit splitting in the ground configuration $3d$ is predicted rather well, achieving an accuracy of 1.3% in Ni^{9+}. It is interesting to note that our calculated results correctly reproduce the observed inversion of the $3d_J$ levels in K. As pointed out by Detrich and Weiss,[31] the j-j single-configuration relativistic wave function partially includes core polarization effects which are usually invoked to explain the inversion. The model wave function correctly predicts that the core polarization is not strong enough to cause inversion along the isoelectronic sequence.

In Fig. 3 we illustrate the Z dependence of the difference between experimental and theoretical spin-orbit splitting of the $3d\ ^2D_J$ levels. This difference consists of two effects incompletely represented by our single-configuration Dirac-Fock calculation, namely electron correlation in the core and higher-order relativistic effects, including terms that couple electron correlation with relativity. The leading Z dependence of the (nonrelativistic) electron correlation deficient in our theory is Z^0 and Z^{-1}. The leading Z dependence of the relativistic contribution to energy levels are $(Z\alpha)^2$ and $(Z\alpha)^4$, where α is the fine-structure constant. Hence, we expect the Z dependence of the terms missing in our theory to be $aZ^0+bZ+cZ^2+\cdots$. In Fig. 3 we find that Z^0 term prevails for $Z \leq 25$, and then the difference increases as Z increases. The experimental values for Zn^{11+} and Se^{15+} seem not to be conform to the trend indicated by the experimental values[28] for Zr^{21+} and Mo^{23+}. Additional experimental data for $Z=30-40$ are needed to verify the Z dependence of this difference for $Z \geq 30$.

We find that the main mode of decay of the $4s\ ^2S_{1/2}$ level is by electric quadrupole radiation to the $3d\ ^2D_{3/2}$ and $3d\ ^2D_{5/2}$ levels, magnetic dipole transition to $3d\ ^2D_{5/2}$ being not allowed. The magnetic dipole transition probability between the $4s\ ^2S_{1/2}$ and $3d\ ^2D_{3/2}$ levels is very small indeed, as expected, and makes only a minor contribution to the decay of the upper state. However, the probability increases 10 000-fold from K to Cr^{5+}. Thus decay by magnetic dipole radiation may become important for members of the isoelectronic sequence of high nuclear charge.

It is interesting to note that both the magnetic dipole and electric quadrupole transition probabilities pass through a minimum for Ca^+. This is due to two factors: (a) the lowering of transition energy as the $4s\ ^2S_{1/2}$ and $3d\ ^2D_J$ levels switch relative positions as a function of nuclear charge from K to Sc^{2+} and (b) magnetic dipole and electric quadrupole line strengths apparently pass through a minimum at Ca^+ as a function of nuclear charge. The magnitude of A_{E2} values suggests that such electric quadrupole lines may be strong enough to be detected from Ti^{3+} and beyond. Furthermore, the difference (about 50%) in A_{E2} values for the $4s\ ^2S_{1/2}-3d\ ^2D_{3/2}$ and $4s\ ^2S_{1/2}-3d\ ^2D_{5/2}$ transitions except for K and Ca^+ shows that relativistic effects may not be negligible even for low Z.

We note in Table IV that the magnetic dipole transition probability between the $4s\ ^2S_{1/2}$ and $3d\ ^2D_{3/2}$ levels passes through a minimum for Zn^{11+} as nuclear charge increases. This is caused by a cancellation of positive and negative contributions to the relevant transition integral resulting in an unusually small value as evidenced by the change of sign of the transition integral from Cu^{10+} to Ga^{12+} through Zn^{11+}. There are hardly any experimental values for A_{E2} or A_{M1} to be compared with theoreti-

cal values except for K. For K, Hertel and Ross[22] obtained experimentally for A_{E2} ($3d\ ^2D_{5/2}$–$4s\ ^2S_{1/2}$) a value of 310±60 sec^{-1} compared to previously published[13] theoretical values of 142.3, 103.6, and 130 sec^{-1}. We obtain a value of 154.2 sec^{-1} in the present calculation. Hertel and Ross may have overestimated A_{E2} as the validity of the Born approximation assumed in interpreting the data in the energy range studied is open to question. However, we believe our values for higher members of the K isoelectronic sequence may be of satisfactory accuracy as valence-core correlation becomes negligible as nuclear charge increases. Further experimental study particularly of higher members of the sequence is highly desirable.

Calculated electric quadrupole and magnetic dipole transition probabilities between the $3d\ ^2D_{5/2}$ and $3d\ ^2D_{3/2}$ levels shown in Table V suggest that magnetic dipole radiation emission is the dominant decay process, the magnetic dipole transition probability being larger than the electric quadrupole transition probability by a factor ranging from 10^8 to 10^5.

IV. CONCLUSION

Our calculated results predict that the dominant mode of decay of the $4s\ ^2S_{1/2}$ level to the $3d\ ^2D_J$ levels is by electric quadrupole radiation as compared to the competing magnetic dipole radiation and that the $4s\ ^2S_{1/2}$ level is certainly metastable in Mn^{6+}, Fe^{7+}, Co^{8+}, and Ni^{9+}. It may be quite possible to detect such electric quadrupole radiations for Mn^{6+}, Fe^{7+}, Co^{8+}, and Ni^{9+} in tokamak plasmas. Metastability of the $4s\ ^2S_{1/2}$ level in higher members of the sequence is open to question and must await determination of the location of odd-parity core-excited states theoretically or experimentally.

Fine-structure splitting between the $3d\ ^2D_J$ levels has been calculated. The calculated values are in good agreement with those which are known experimentally. The $3d\ ^2D_{5/2}$ level is predicted to decay to the $3d\ ^2D_{3/2}$ level mainly by magnetic dipole radiation and the corresponding magnetic dipole radiation may be observable for Mo^{23+}, Nb^{22+}, Zr^{21+}, and other ions of the sequence. We have used simplified model wave functions in these calculations, neglecting electron correlation in the core. However, electron correlation would be expected to be less important for the higher members of the sequence but might be more important towards the neutral end of the sequence. We are currently investigating the effect of incorporation of electron correlation within the MCDF approach on transition energies and transition probabilities as a part of the general study of the energy-level structure of the potassium isoelectronic sequence.

ACKNOWLEDGMENTS

We wish to thank Dr. A. W. Weiss for sharing his unpublished results on the K sequence and for useful discussions and suggestions and Dr. J. P. Desclaux for allowing us to use the MCDF programs. A gift of free computer time from the Howard University Computer Center and systems programming help from Curtis Butler in adapting the MCDF programs for the IBM 3090 are gratefully acknowledged. One of us (M.A.A.) would like to thank the National Bureau of Standards for providing research support. This work was partly supported by the Office of Fusion Energy, U.S. Department of Energy.

[1]D. E. Osterbrock, *Astrophysics of Gaseous Nebulae* (Freeman, San Francisco, 1974).
[2]A. H. Gabriel and C. Jordan, Mon. Not. R. Astron. Soc. **145**, 241 (1969).
[3]B. Edlén, Phys. Scr. **T8**, 5 (1984).
[4]S. Suckewer and E. Hinnov, Phys. Rev. A **20**, 578 (1979).
[5]S. Suckewer, R. Fonck, and E. Hinnov, Phys. Rev. A **21**, 924 (1980).
[6]E. Hinnov and S. Suckewer, Phys. Lett. **32A**, 298 (1980).
[7]R. D. Cowan, *The Theory of Atomic Structure and Spectra* (University of California Press, Berkeley, 1981).
[8]V. Kaufman and J. Sugar, J. Phys. Chem. Ref. Data **15**, 321 (1986).
[9]J. C. Gauthier, J. P. Geindre, P. Monier, E. Luc-Koenig, and J. F. Wyart, J. Phys. B **19**, L385 (1986).
[10]M. Godefroid, C. E. Magnusson, P. O. Zetterberg, and I. Joelsson, Phys. Scr. **32**, 125 (1986).
[11]C. E. Tull, M. Jackson, R. P. McEachran, and M. Cohen, Can. J. Phys. **50**, 1169 (1972).
[12]E. Biemont and M. Godefroid, Phys. Scr. **18**, 323 (1978).
[13]S. R. Langhoff, C. W. Bauschlicher, and H. Partridge, J. Phys. B **18**, 13 (1985).
[14]M. Godefroid and G. Verhaegen, J. Phys. B **13**, 3081 (1980).
[15]S. Chung, C. C. Lin, C. F. Fischer, and E. T. P. Lee, J. Chem. Phys. **76**, 498 (1982).
[16]S. Sengupta, J. Quant. Spectrosc. Radiat. Transfer **15**, 159 (1975).
[17]D. R. Beck, Phys. Rev. A **23**, 159 (1981).
[18]K. T. Cheng, Y.-K. Kim, and J. P. Desclaux, At. Data Nucl. Data Tables **24**, 111 (1979).
[19]K.-N. Huang, At. Data Nucl. Data Tables **32**, 503 (1985).
[20]J. Sugar and C. Corliss, J. Phys. Chem. Ref. Data **14**, 1 (1985).
[21]R. H. Garstang, in *Atomic and Molecular Processes,* edited by D. R. Bates (Academic, New York, 1962).
[22]I. V. Hertel and K. J. Ross, J. Phys. B **2**, 285 (1969).
[23]J. P. Desclaux, Comput. Phys. Commun. **9**, 31 (1975); an improved version developed by J. P. Desclaux and Y.-K. Kim (unpublished) was used for the present calculations.
[24]A. A. Ramonas and A. N. Ryabtsev, Opt. Spectrosc. **48**, 631 (1980).
[25]M. W. D. Mansfield, N. J. Peacock, C. C. Smith, M. G. Hobby, and R. D. Cowan, J. Phys. B **11**, 1521 (1978).
[26]J. Sugar and V. Kaufman, Phys. Scr. **34**, 797 (1986).
[27]J. Sugar, V. Kaufman, and W. L. Rowan, J. Opt. Soc. Am. B **5**, 236 (1988).
[28]S. Suckewer, E. Hinnov, S. Cohen, M. Finkenthal, and K. Sato, Phys. Rev. A **26**, 1161 (1982).
[29]L. I. Sobelman, *Introduction to the Theory of Atomic Spectra* (Pergamon, Oxford, 1972), Sec. 32.
[30]S. J. Czyzak and T. K. Krueger, Astrophys. J. **144**, 381 (1966).
[31]J. Detrich and A. W. Weiss, Phys. Rev. A **25**, 1203 (1982).